

Magnetic monopoles in the high temperature phase of Yang–Mills theories

A. D’Alessandro and M. D’Elia*

*Dipartimento di Fisica, Università di Genova and INFN, Sezione di Genova,
Via Dodecaneso 33, I-16146 Genova, Italy***Abstract**

We investigate the properties of thermal abelian magnetic monopoles in the high temperature phase of Yang–Mills theories, following a recent proposal for their identification on lattice configurations. The study is done for SU(2) pure gauge theory, for temperatures going up to about 10 times the deconfining temperature and using the Maximal Abelian gauge to perform the abelian projection. We find that the monopole density has a well defined continuum limit. Its temperature dependence disagrees with a free particle gas prediction and is instead well described by a $T^3/(\log(T/\Lambda))^\alpha$ behaviour in all the explored range, with $\alpha \sim 2$ and $\Lambda \sim 100$ MeV. Also the study of spatial correlations of thermal monopoles shows the presence of non-trivial interactions among them. Finally, we discuss the gauge dependence of our results, showing that it is significant and that, even within the Maximal Abelian gauge, Gribov copy effects are important.

I. INTRODUCTION

Abelian magnetic monopoles are topological defects which may be relevant for many non-perturbative features of QCD. They enter for instance in the mechanism for color confinement based on dual superconductivity of the vacuum [1–3], which relates confinement to the spontaneous breaking of a magnetic symmetry induced by monopole condensation: the magnetic condensate disappears at the deconfining phase transition, as lattice simulations have shown extensively [4–9].

Magnetically charged particles have also been proposed to be an important component of deconfined matter above the phase transition [10–14], possibly contributing to the physical properties of the strongly interacting Quark-Gluon Plasma. In Ref. [13] the magnetic component of the deconfined plasma has been directly related to thermal abelian monopoles evaporating from the magnetic condensate which is present at low temperatures; moreover it has been proposed to detect such thermal monopoles in finite temperature lattice QCD simulations by identifying them with monopole currents having a non-trivial wrapping in the Euclidean temporal direction [13,15,16]. First numerical investigations of these wrapping trajectories were performed in Ref. [15] and [16].

*E-mail addresses: adales@ge.infn.it, delia@ge.infn.it

The purpose of this paper is to work on this last proposal and perform a detailed study of the properties of thermal abelian monopoles. We will verify if the density of such thermal objects is a well defined physical quantity, i.e. independent of the lattice UV cut-off in the continuum limit, determine its temperature dependence, compare it with phenomenological models and study the spatial distribution of the wrapping trajectories. To that aim we have performed extensive numerical simulations of pure $SU(2)$ lattice gauge theory in the deconfined region, in a range of temperatures going up to $\sim 10 T_c$.

Abelian monopole currents are exposed on the lattice by the usual De Grand - Tous-saint procedure [17]. That is done on abelian projected configurations, meaning that the so exposed monopole currents are gauge dependent quantities. The usual attitude in the literature is to define and study monopole currents in the gauge which maximizes the abelian component of Yang-Mills fields, the so-called Maximal Abelian gauge (MAG), the rationale being that in this way abelian projected fields reproduce most of the original Yang-Mills dynamics (Abelian Dominance). We have followed that recipe in our study. However we believe that the problem of gauge dependence is particularly important, especially if one wants to associate the so detected thermal abelian monopoles with real thermal objects influencing the physical properties of the Quark-Gluon Plasma: for that reason part of our investigation has been dedicated to this issue.

The paper is organized as follows. In Section II we illustrate our numerical simulations and present results about the density and the spatial correlation of wrapping monopole trajectories. In Section III we investigate the gauge dependence of our results. Finally, in Section IV, we draw our conclusions.

II. NUMERICAL SIMULATIONS AND RESULTS

We have performed numerical simulations of $SU(2)$ pure gauge theory, using the standard plaquette action and various lattice sizes $L_s^3 \times L_t$ at different values of the inverse gauge coupling $\beta = 2N_c/g^2$. The physical scale has been determined according to $a(\beta)\Lambda_L = R(\beta)\lambda(\beta)$, where R is the two-loop perturbative β -function, while λ is a non-perturbative correction factor computed and reported in Ref. [18]. Finally, the values $T_c/\Lambda_L = 21.45(14)$ and $T_c/\sqrt{\sigma} = 0.69(2)$ have been assumed respectively from Ref. [18] and [19], where T_c is the deconfining critical temperature.

Abelian monopole currents are identified by the De Grand-Toussaint construction [17] after abelian projection, the last procedure requiring gauge fixing. Following the attitude adopted by previous literature, we have worked in the Maximal Abelian gauge (MAG), defined by maximizing the following functional with respect to gauge transformations:

$$F_{\text{MAG}} = \sum_{\mu, x} \text{Re tr} \left[U_\mu(x) \sigma_3 U_\mu^\dagger(x) \sigma_3 \right] \quad (2.1)$$

which is proportional to the average squared diagonal part of the gauge links. It can be shown that on stationary points of the MAG functional the local operator

$$X(x) = \sum_{\mu} \left[U_\mu(x) \sigma_3 U_\mu^\dagger(x) + U_\mu^\dagger(x - \mu) \sigma_3 U_\mu(x - \mu) \right] \quad (2.2)$$

is diagonal. The maximization of the MAG functional on a given configuration has been achieved by an iterative combination of local maximization and overrelaxation (see Ref. [20]),

stopping the algorithm when the average squared modulus of the non-diagonal part of $X(x)$ was less than a given parameter ω [20]. We have chosen $\omega = 10^{-8}$ (see Section III for a discussion about the dependence on ω).

After taking the diagonal part of gauge links on the gauge fixed configuration (abelian projection), monopole currents are defined as [17]:

$$m_\mu = \frac{1}{2\pi} \varepsilon_{\mu\nu\rho\sigma} \hat{\partial}_\nu \bar{\theta}_{\rho\sigma} \quad (2.3)$$

where $\bar{\theta}_{\rho\sigma}$ is the compactified part of the abelian plaquette phase

$$\theta_{\mu\nu} = \bar{\theta}_{\mu\nu} + 2\pi n_{\mu\nu} \quad (2.4)$$

and $n_{\mu\nu} \in \mathbf{N}$.

Monopole currents form closed loops, since $\hat{\partial}_\mu m_\mu = 0$. These loops may be either topologically trivial or wrapped around the lattice. Following the proposal in Refs. [13,15,16], among different currents we select those having a non-trivial wrapping around the euclidean temporal direction, identifying them with thermal monopoles. This procedure identifies at any given timeslice the number and the spatial positions of the wrapping trajectories. The thermal monopole density is then defined as [13,15,16]

$$\rho = \frac{\langle \sum_{\vec{x}} |N_{wrap}(m_0(\vec{x}, t))| \rangle}{V_s} \quad (2.5)$$

where $N_{wrap}(m_0(\vec{x}, t))$ is the temporal winding number of the monopole current m_0 at site (\vec{x}, t) , while $V_s = (L_s a)^3$ is the spatial volume.

A. Monopole density

We have performed an extensive study of the thermal monopole density defined in Eq. (2.5), in a range of temperature going from $\sim 1.3 T_c$ to about $10 T_c$. In particular, in order to study the dependence both on the temperature and on the UV cutoff, we have done 4 different sets of simulations with parameters $(L_s, \beta) = (24, 2.5115), (32, 2.6), (40, 2.7)$ and $(48, 2.75)$, corresponding to different lattice spacings but approximately equal spatial sizes $L_s a(\beta) \sim 2$ fm. For each set we have performed simulations with different values of L_t (ranging from 4 to $L_s/4$), corresponding to different temperatures $T = 1/(L_t a)$. A further set of simulations has been done on a $48^3 \times 4$ lattice and inverse gauge couplings up to $\beta = 3.10$, in order to extend the range of temperatures explored. Accumulated statistics range from about 500 decorrelated configurations for the largest lattices $L_s = 48$ to about $5 \cdot 10^3$ for the smallest lattices $L_s = 24$. All results are reported in Table I, both in adimensional and in physical units.

We have carefully verified the absence of finite volume effects. We show two examples in Fig. 1, where the dependence of ρa^3 on the spatial size is plotted as a function of L_s for two different combinations of β and L_t : in both cases the value of L_s used to extract our data is well within an extended plateau region. A similar check has been performed for the dependence on the gauge fixing stopping parameter ω : a detailed discussion about gauge dependence is reported in Section III. We have also checked the absence, in the

whole temperature range explored, of trajectories wrapping in a spatial instead than in the temporal direction.

Let us now discuss the dependence of our results on the UV cut-off. We report in Fig. 2 results obtained for ρ versus T/T_c for 4 different values of the lattice spacing. The physical scale has been determined as discussed above and fixing $\sqrt{\sigma} = 430$ MeV. The agreement among data obtained at different UV cut-off is reasonable, indicating that the density of wrapping monopole trajectories has a well defined continuum limit.

Next we turn to the temperature dependence of ρ . The thermal distribution for a gas of free ultrarelativistic (massless) scalar particles predicts a density:

$$\int \frac{d^3\vec{p}}{(2\pi)^3} \frac{1}{\exp(|\vec{p}|/T) - 1} = \frac{\zeta(3)}{\pi^2} T^3. \quad (2.6)$$

The behaviour $\rho(T) \propto T^3$ is expected anyway in the $T \rightarrow \infty$ limit if the monopoles can be considered as asymptotically free in that regime. We report in Fig. 3 the adimensional ratio $\rho/T^3 = \rho(aL_t)^3$ versus T/T_c , for the data on our biggest spatial size ($L_s = 48$) and $\beta \geq 2.75$; notice that ρ/T^3 is not influenced by the systematic error related to the determination of the physical scale, which only affects T/T_c , hence the horizontal scale of Fig. 3. It is apparent from the figure that the behaviour $\rho \propto T^3$ is not verified in all the explored range, i.e. for temperatures up to $T \sim 10 T_c$. It can be easily realized that the deviation from the simple cubic behaviour cannot be simply explained by the presence of a finite monopole mass m_M , i.e. by correcting $|\vec{p}| \rightarrow \sqrt{|\vec{p}|^2 + m_M^2}$ in the expression of the free particle energy in Eq. (2.6): indeed ρ/T^3 would be an increasing function of T in that case, in clear contrast with the behaviour visible in Fig. 3.

We conclude that the description of thermal monopoles as a gas of free particles is not appropriate, and interactions must be taken into account also at very high temperatures. That is in agreement with the scenario of an electric dominated phase for Yang–Mills theories at very high temperatures, in which the magnetic component is strongly interacting [11]. Predictions have been made for the density of magnetic objects [21], based on perturbative and dimensional reduction considerations, leading to a behaviour like $g^6 T^3$, hence a reduction factor with respect to the free massless particle case of the order of $1/(\log(T/\Lambda))^3$; similar predictions have been reported in Ref. [11].

Based on that, we have tried to correct the cubic behaviour as follows:

$$\frac{\rho}{T^3} = \frac{A}{(\log(T/\Lambda_{eff}))^\alpha} \quad (2.7)$$

and we have verified that this simple correction describes very well our data in all the explored range. In particular, a fit including data with $T > 2 T_c$ leads to $A = 0.48(4)$, $T_c/\Lambda_{eff} = 2.48(3)$ and $\alpha = 1.89(6)$, with $\chi^2/\text{d.o.f.} = 10.6/12$. Results do not change much if the range of fitted points is changed, with α always compatible or marginally compatible with 2 and $\chi^2/\text{d.o.f.}$ of order 1. If we fix $\alpha = 2$ we obtain $A = 0.557(10)$, $T_c/\Lambda_{eff} = 2.69(3)$ (i.e. $\Lambda_{eff} \sim 110$ MeV) and $\chi^2/\text{d.o.f.} = 13.7/13$ for data corresponding to $T > 2 T_c$; results are completely stable within errors if the fitted temperature range is changed, with only a slight increase in $\chi^2/\text{d.o.f.}$ (up to 23/17) if temperatures down to $\sim 1.4 T_c$ are included. If we instead fix $\alpha = 3$, reasonable fits are obtained for $T > 5 T_c$, while $\alpha = 1$ seems to be excluded by our data.

We conclude that the simple ansatz in Eq. (2.7) perfectly describes our data, with $\alpha \sim 2$, for all temperatures ranging from $T \sim 2 T_c$ up to $T \sim 10 T_c$ and with Λ_{eff} of the order of Λ_{QCD} . In order to better appreciate that, we have plotted in Fig. 4 the quantity $(\rho/T^3)^{-1/2}$ versus $\log(T/T_c)$: the dependence is manifestly linear, as Eq. (2.7) predicts in the case $\alpha = 2$.

B. Monopole interactions

In order to further investigate the interactions existing among wrapped monopole trajectories, we have studied their distribution at a fixed time slice, so as to obtain information about the spatial correlation of thermal monopoles. In particular we have determined the density–density correlation function $g(r) \equiv \langle \varrho(0)\varrho(r) \rangle / \varrho^2$, which can also be measured (for $r \neq 0$) as the ratio between the probability of having a particle at a distance r from a given reference particle and the same probability in a completely homogeneous system, in practice

$$g(r) = \frac{1}{\varrho} \frac{dN(r)}{4\pi r^2 dr} \quad (2.8)$$

where $dN(r)$ is the number of particles in a spherical shell of thickness dr at distance r from the reference particle and by ϱ we mean the average density of such particles (monopoles or antimonopoles). A value $g(r) < 1$ ($g(r) > 1$) indicates that at distance r we have less (more) particles than expected in a non-interacting medium, i.e. there is a repulsive (attractive) interaction. In our numerical study we have used, in place of $4\pi r^2 dr$, the actual number of lattice sites contained in the shell, in order to take into account part of the discretization effects.

We have measured $g(r)$ for both the monopole-monopole and the monopole-antimonopole case in some of our simulations. In Fig. 5 we show the results obtained at $\beta = 2.7$ on a lattice with $L_s = 40$ and $L_t = 5$ ($T \simeq 2.85 T_c$) on a set of 300 decorrelated configurations. $g(r)$ is clearly depleted at short distances in the monopole-monopole case, indicating a repulsive interaction. On the contrary $g(r)$ is enhanced at short distance in the monopole-antimonopole case, indicating an attractive interaction. Actually in this last case (monopole-antimonopole) $g(r)$ has a peak at distances of about 0.2 fm (4 lattice spacings) and then goes down again, reaching values < 1 : that could either be related to finite lattice spacing effects or have a physical meaning.

This is an important issue that must be clarified, therefore we have decided to repeat the measurements on a lattice with $L_s = 64$ and $L_t = 8$ at $\beta = 2.86$: we have $a(\beta = 2.86)/a(\beta = 2.7) \simeq 5/8$ within a good precision, hence the new measurements correspond to equal physical volume and temperature but different UV cutoff. Also in this case we have collected a set of 300 decorrelated configurations. Results are reported again in Fig. 5, the distance r is reported in physical units so that comparison is straightforward. A nice scaling to the continuum limit can be appreciated, apart from results obtained at a distance of ~ 1 lattice spacing. In particular we can confirm that the peak observed in the monopole-antimonopole correlation at ~ 0.2 fm is not a lattice artifact but the signal of more structured interaction patterns.

In Fig. 6 we illustrate some results regarding the temperature dependence of monopole interactions. The function $g(r)$ shows appreciable changes as T is varied, even if not dramatic

from a qualitative point of view. In particular the peak in the monopole-antimonopole correlation function moves to larger distances as T is lowered.

In the large distance region, where $g(r) \simeq 1$, one can try to extract direct information about the interaction potential $V(r)$ based on the ansatz (and assuming $V(\infty) = 0$):

$$g(r) \simeq \exp(-V(r)/T) \quad (2.9)$$

We have tried this strategy, finding that $V(r)$ can be described reasonably well by a Yukawa potential (two sample fits are reported in Fig. 5)

$$V(r) \propto \frac{e^{-\lambda_P r}}{r} \quad (2.10)$$

with a plasma screening length λ_P of the order of 0.1 fm.

III. GAUGE DEPENDENCE

We now discuss the issue of gauge dependence. The fact that monopole currents identified by abelian projection are gauge dependent is well known: much likely that applies also to monopole currents wrapping in the temporal direction. A way to detect this phenomenon is to study the dependence of the measured thermal monopole density ρ on the gauge fixing stopping parameter ω : larger values of ω correspond to a looser gauge fixing. An example of such study is reported in Fig. 7, corresponding to $L_s = 32$, $L_t = 4$ and $\beta = 2.6$. When the gauge is poorly fixed the monopole density is larger: a possible interpretation could be that much more ultraviolet noise contributes to the monopole currents in this case, whose effect is that of mimicking in some case the presence of additional wrapping trajectories. However the density is well stable for $\omega < 10^{-7}$.

In all the simulations discussed above we have taken $\omega = 10^{-8}$, if a looser criterion is chosen then the continuum scaling of the monopole density, which is approximately verified on our data shown in Fig. 2, is lost. To show an example of that, we have reported in Table I two values of the density ρ , signalled by a star in the last column, obtained with a stopping criterion $\omega = 10^{-3}$ on two lattices with different UV cutoff but approximately equal physical temperatures: quite different value are obtained for ρ , contrary to what obtained by fixing the gauge more carefully.

What we have shown seems to indicate that thermal monopoles populating the Quark-Gluon Plasma can be indeed identified in lattice simulations and that their density is a well defined physical quantity as soon as a careful gauge fixing is performed. However one may wonder how results change if a different gauge is chosen, in place of MAG, to perform the Abelian projection. The answer is that results change in a dramatic way: an extreme case is provided by Landau gauge, which on the lattice is defined by maximizing the following functional

$$F_L = \sum_{\mu, x} \text{Re tr } U_\mu(x). \quad (3.1)$$

We have repeated part of our measurements in Landau gauge, obtaining exactly zero wrapping monopole trajectories in all the explored cases. That may sound as a warning, nevertheless one could still suppose that the Maximal Abelian gauge has the virtue of correctly

identifying the magnetic component of the Yang–Mills plasma in the form abelian magnetic monopoles. We have however a further warning.

We have tried the following experiment, which is not new and has been performed previously in the literature, even if mostly in the context of center dominance studies [22–25]. We have repeated part of our measurements, using again the Maximal Abelian gauge in order to define the abelian projection, but using a sample of configurations which had been previously fixed to Landau gauge. The result is that thermal abelian monopoles, which are completely absent in Landau gauge, do reappear when fixing again to MAG. However the average monopole density is appreciably lower and, what is worse, scaling to the continuum limit is lost. All that is apparent from Fig. 8. What is more striking is that gauge configurations which are fixed to MAG after Landau gauge fixing (and which show no continuum scaling) reach on average higher values of the MAG functional as compared to original configurations (where instead scaling is observed), as shown for a few examples in Table II.

All that exposes quite clearly the problem of Gribov copies. While looking for the global maximum of the MAG functional in Eq. (2.1) along the gauge orbit of a given configuration, several local maxima are met where a gauge fixing algorithm like the one used by us may stop. All these local maxima have a different content of thermal abelian monopoles, but on average they furnish a monopole density that scales correctly in the continuum limit. If however one starts the same algorithm from points of the gauge orbit corresponding to local maxima of the Landau functional, one reaches local maxima of the MAG functional that, most of the times, are closest in value to the global maximum but have a quite different monopole content which, if continuum scaling is taken as a criterion, one would say to be wrong.

As we have emphasized above, very similar problems are met when studying center dominance in the maximal center gauge (MCG) [22–25] and some possible interpretations have been discussed [24,26]. One should also study how the problem is related to the choice of a particular starting point on the gauge orbit (belonging to Landau gauge in our case) and perform more extensive studies in which the global maximum of the MAG functional is searched for via better algorithms, like for instance simulated annealing [27]. Our opinion is that much has still to be clarified in this context and that the issue of gauge dependence is even more urgent in this case, if one wants to associate wrapping monopole trajectories with real thermal objects populating the Quark-Gluon Plasma.

IV. CONCLUSIONS

Magnetic monopoles may be an important component of the Quark-Gluon Plasma [10–14]. In the present work we have followed a recent proposal aimed at identifying the magnetic component of the high temperature phase of Yang-Mills theories with thermal abelian monopoles detected on lattice configurations in terms of monopole trajectories wrapping in the euclidean temporal direction [13,15,16]: our purpose has been that of investigating the temperature and UV cut-off dependence of the density of thermal monopoles and to study their interactions in the case of $SU(2)$ pure gauge theory. Abelian monopole currents have been identified in the Maximal Abelian gauge, therefore part of our efforts have been dedicated to the issue of gauge dependence: we have shown that it is indeed significant and our physical results should be considered in that light.

We have determined the monopole density ρ in a wide range of temperatures, going from $\sim 1.3 T_c$ to $\sim 10 T_c$, and for different values of the lattice spacing. We have verified a reasonable scaling of ρ to the continuum limit. Regarding the temperature dependence, our data show that ρ is not compatible with a (massive or massless) free particle behaviour in the whole range of temperatures explored. This is in agreement with the picture of an electric dominated phase for Yang–Mills theories at very high temperatures, in which the magnetic component is strongly interacting [11]. Inspired by that picture and by predictions based on perturbative computations and dimensional reduction [21], we have tried to fit our data according to $\rho \propto T^3/(\log T/\Lambda_{eff})^\alpha$, finding that a coefficient $\alpha = 2$ and $\Lambda_{eff} \sim 100$ MeV describe perfectly our data in all the explored temperature range. A coefficient $\alpha = 3$ is not excluded for $T > 5 T_c$.

By studying the distribution of wrapping monopole trajectories at a given timeslice, we have extracted information about density–density spatial correlation functions both in the monopole–monopole and in the monopole–antimonopole case. We have thus verified the presence of a repulsive (attractive) interaction at large distances, in agreement with a screened Coulomb potential and a screening length of the order of 0.1 fm. Repulsion is observed at short distances in both cases, with a peak in the monopole–antimonopole correlation function at a distance which we have verified to scale well to the continuum limit and which is about 0.15 fm at $T \simeq 3.85 T_c$ and goes up to ~ 0.4 fm close to the critical temperature. More extensive future studies could better clarify the nature of the interaction, both in the high T region and closer to T_c , where one could search for a possible interplay with the dynamics of the deconfinement transition. Of course the extension of our results to $SU(3)$ pure gauge theory will be the natural continuation of our study.

Let us stress once again that all results apply to thermal abelian monopoles identified in a particular gauge. As we have shown in our study presented in Section III, results are strongly gauge dependent, an extreme case being Landau gauge, where thermal abelian monopoles completely disappear. This dependence is well known and the Maximal Abelian gauge has been always considered as a special gauge in which abelian monopoles are better identified. Moreover, we have shown that Gribov copy effects may change results even within a given gauge, if particular points are chosen along the gauge orbit where the gauge fixing procedure is started. We have considered the example of the Maximal Abelian gauge fixed starting from local maxima of the Landau functional: higher maxima of the MAG functional are reached but the continuum scaling of the monopole density is lost. One should study how this problem is related to the particular starting point on the gauge orbit and perform more extensive studies, looking for the global maximum of the MAG functional via dedicated algorithms like simulated annealing [27].

In conclusion, our opinion is that if one really wants to associate thermal abelian monopoles with (part of) the magnetic component of the Quark-Gluon Plasma, the issue of gauge dependence should be better clarified: more numerical and theoretical efforts have to be done in this respect.

ACKNOWLEDGMENTS

We thank C. M. Becchi, V. Bornyakov, M. Chernodub, A. Di Giacomo, C. Korthals-Altes, E. Shuryak and V. Zakharov for many interesting discussions. We would also like to

thank A. Brunengo and M. Corosu for their kind technical support in the use of the PC farm at INFN - Genova, where numerical simulations have been performed.

REFERENCES

- [1] G. 't Hooft, in “High Energy Physics”, EPS International Conference, Palermo 1975, ed. A. Zichichi.
- [2] S. Mandelstam, Phys. Rept. **23**, 245 (1976).
- [3] G. Parisi, Phys. Lett. **B60**, 93 (1975).
- [4] A. Di Giacomo, B. Lucini, L. Montesi, G. Paffuti, Phys. Rev. **D 61**, 034503 (2000) [arXiv:hep-lat/9906024]; Phys. Rev. **D 61**, 034504 (2000) [arXiv:hep-lat/9906025];
- [5] J. M. Carmona, M. D’Elia, A. Di Giacomo, B. Lucini, G. Paffuti, Phys. Rev. **D 64**, 114507 (2001) [arXiv:hep-lat/0103005];
- [6] J. M. Carmona, M. D’Elia, L. Del Debbio, A. Di Giacomo, B. Lucini, G. Paffuti, Phys. Rev. **D 66**, 011503 (2002) [arXiv:hep-lat/0205025];
- [7] M. D’Elia, A. Di Giacomo, B. Lucini, G. Paffuti, C. Pica, Phys. Rev. **D 71**, 114502 (2005) [arXiv:hep-lat/0503035].
- [8] M.N. Chernodub, M.I. Polikarpov and A.I. Veselov, Phys. Lett. **B399**, 267 (1997).
- [9] P. Cea and L. Cosmai, JHEP **0111**, 064 (2001); P. Cea, L. Cosmai and M. D’Elia, JHEP **0402**, 018 (2004).
- [10] C. P. Korthals Altes, hep-ph/0607154.
- [11] J. Liao, E. Shuryak, Phys. Rev. **C 75** 054907 (2007) [hep-ph/0611131].
- [12] J. Liao, E. Shuryak, arXiv:0706.4465 [hep-ph].
- [13] M. N. Chernodub and V. I. Zakharov, Phys. Rev. Lett. **98**, 082002 (2007) [arXiv:hep-ph/0611228]; M. N. Chernodub and V. I. Zakharov, arXiv:hep-ph/0702245.
- [14] M. N. Chernodub, K. Ishiguro, A. Nakamura, T. Sekido, T. Suzuki and V. I. Zakharov, arXiv:0710.2547 [hep-lat].
- [15] V.G. Bornyakov, V.K. Mitrjushkin and M. Muller-Preussker Phys. Lett. **B284**, 99 (1992).
- [16] S. Ejiri, Phys. Lett. **B376**, 163 (1996) [arXiv:hep-lat/9510027].
- [17] A. De Grand, D. Toussaint, Phys. Rev. **D 22** 2478 (1980).
- [18] J. Engels, F. Karsch, K. Redlich, Nucl. Phys. **B 435**, 295 (1995) [arXiv:hep-lat/9408009].
- [19] J. Fingberg, U. Heller, F. Karsch, Nucl. Phys. **B 392**, 493 (1992) [arXiv:hep-lat/9208012].
- [20] P. Cea, L. Cosmai Phys. Rev. **D 52**:5152 (1995) [hep-lat/9504008].
- [21] P. Giovannangeli and C. P. Korthals Altes, Nucl. Phys. **B 608**, 203 (2001) [arXiv:hep-ph/0102022].
- [22] T. G. Kovacs, E. T. Tomboulis Phys. Lett. **B463**, 104 (1999) [hep-lat/9905029].
- [23] G. S. Bali, V. Bornyakov, M. Mueller-Preussker, K. Schilling, Phys. Rev. **D 54** 2863 (1996) [hep-lat/9603012]; V. G. Bornyakov, D. A. Komarov, M. I. Polikarpov, Phys. Lett. **B497** 151 (2001).
- [24] M. Faber, J. Greensite, S. Olejnik Phys. Rev. **D 64**, 034511 (2001) [hep-lat/0103030]; M. Faber, J. Greensite, S. Olejnik, D. Yamada, JHEP **9912**, 012 (1999).
- [25] A. O Cais, W. Kamleh, K. Langfeld, B. Lasscock, D. Leinweber, L. von Smekal, arXiv:0710.2958
- [26] V. I. Zakharov, Braz. J. Phys. **37**, 165 (2007) [arXiv:hep-ph/0612342].
- [27] V. G. Bornyakov, D. A. Komarov, M. I. Polikarpov and A. I. Veselov, arXiv:hep-lat/0210047.

TABLES

β	L_s	L_t	$\langle N_{wrap} \rangle / L_s^3$	T/T_c	$\rho(\text{fm}^{-3})$
2.5115	24	6	0.001384(7)	1.333	2.404(12)
2.5115	24	5	0.001916(10)	1.600	3.331(18)
2.5115	24	4	0.002938(10)	2.000	5.107(19)
2.6	32	8	0.000604(4)	1.315	2.387(15)
2.6	32	7	0.000765(4)	1.503	3.025(16)
2.6	32	6	0.001003(3)	1.754	3.969(13)
2.6	32	6	0.001550(5)	1.754	6.135(20) *
2.6	32	5	0.001408(3)	2.105	5.574(13)
2.6	32	4	0.002223(4)	2.631	8.806(25)
2.7	40	10	0.000289(8)	1.424	2.834(8)
2.7	40	9	0.000356(7)	1.582	3.49(7)
2.7	40	8	0.000431(6)	1.780	4.23(6)
2.7	40	8	0.000784(15)	1.780	7.69(15) *
2.7	40	7	0.000549(5)	2.035	5.39(5)
2.7	40	6	0.000734(4)	2.374	7.20(4)
2.7	40	5	0.001050(4)	2.848	10.30(4)
2.7	40	4	0.0016818(29)	3.561	16.50(29)
2.75	48	12	0.0001838(23)	1.377	2.82(4)
2.75	48	11	0.0002157(21)	1.502	3.30(3)
2.75	48	10	0.000249(4)	1.653	3.8(6)
2.75	48	9	0.0003030(22)	1.836	4.64(3)
2.75	48	8	0.000370(3)	2.066	5.67(4)
2.75	48	7	0.000473(3)	2.361	7.25(4)
2.75	48	6	0.000638(4)	2.754	9.77(6)
2.75	48	5	0.000919(4)	3.305	14.08(6)
2.75	48	4	0.001488(5)	4.131	22.80(8)
2.78	48	4	0.001388(4)	4.521	27.87(8)
2.81	48	4	0.001293(4)	4.938	33.83(10)
2.84	48	4	0.001202(4)	5.392	40.95(13)
2.87	48	4	0.001131(5)	5.884	50.07(24)
2.90	48	4	0.001065(5)	6.419	61.2(3)
2.93	48	4	0.001000(5)	7.000	74.5(4)
2.96	48	4	0.000956(5)	7.631	92.3(4)
3.00	48	4	0.000879(4)	8.557	119.7(5)
3.05	48	4	0.000811(5)	9.865	169.2(11)
3.10	48	4	0.000740(4)	11.365	236.0(12)

TABLE I. Monopole density in lattice units (fourth column) and physical units (last column) for different lattice sizes and inverse gauge couplings. In the fifth column we report the corresponding values of T/T_c . In order to determine the physical scale in the last column, we have assumed $\sqrt{\sigma} = 430$ MeV; a star indicates data obtained with a looser gauge fixing criterion $\omega = 10^{-3}$ ($\omega = 10^{-8}$ has been used in all other cases).

$L_s^3 \times L_t$	Landau+ <i>MAG</i>	<i>MAG</i>
$40^3 \times 7$	1.56013(6)	1.55898(7)
$32^3 \times 5$	1.53470(13)	1.53354(14)
$32^3 \times 6$	1.53438(16)	1.53335(17)
$32^3 \times 7$	1.53420(7)	1.53313(6)

TABLE II. Average normalized maximum reached for the MAG functional, Eq. (2.1), during the gauge fixing procedure, with and without performing a previous gauge fixing to Landau gauge.

FIGURES

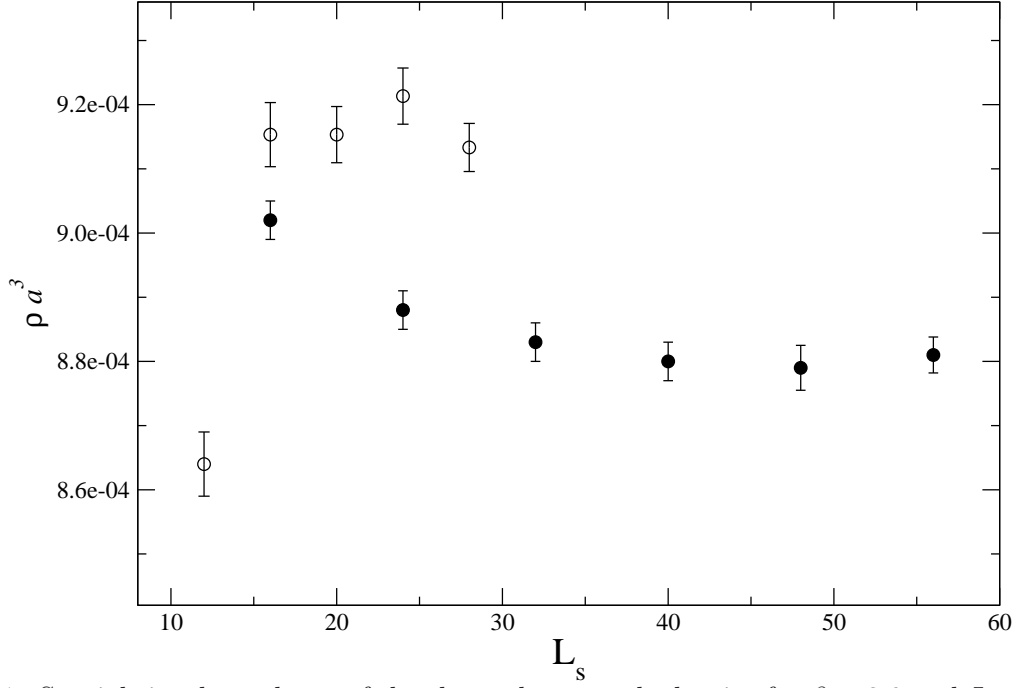


FIG. 1. Spatial size dependence of the thermal monopole density for $\beta = 3.0$ and $L_t = 4$ (filled circles) and for $\beta = 2.5115$ and $L_t = 6$ (blank circles). In the last case data have been divided by a factor 1.5 to fit in the figure. The corresponding data reported in Table I have been obtained for $L_s = 24$ and $L_s = 48$ respectively, i.e. well within the two plateau regions.

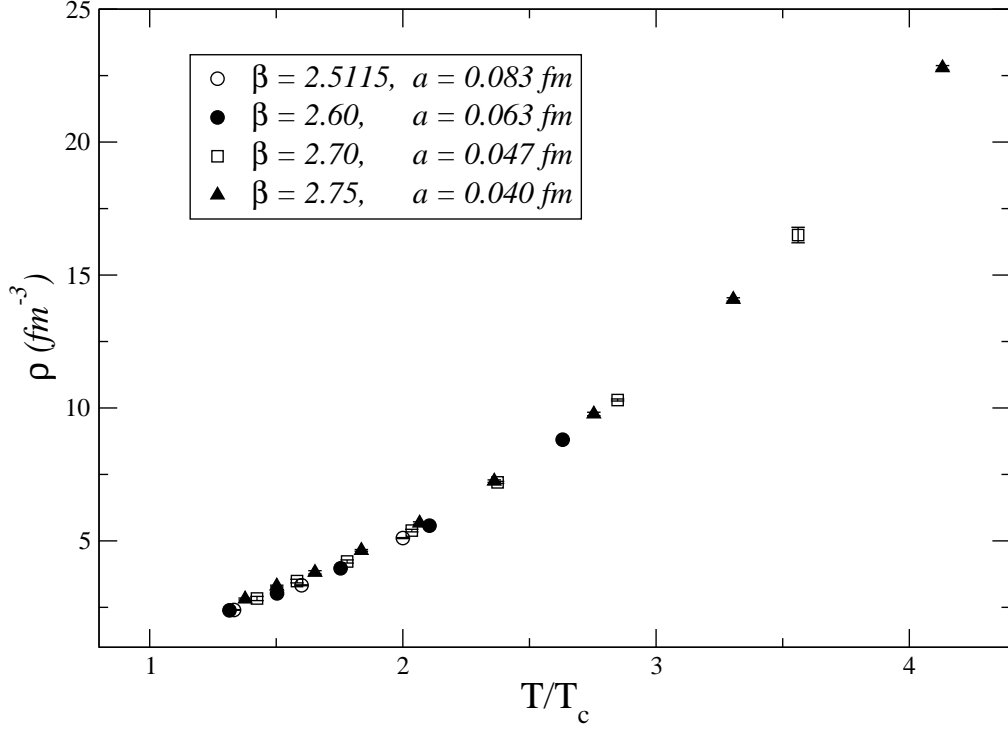


FIG. 2. Monopole density $\rho(T)$ in fm^{-3} for different values of T and different lattice spacings.

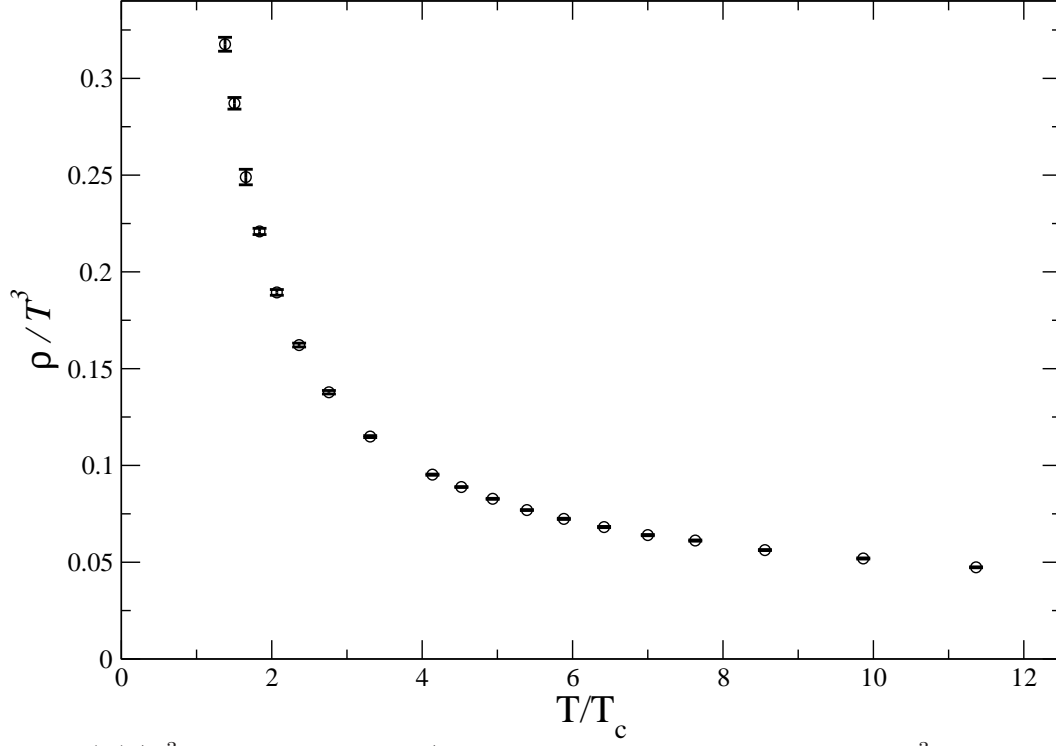


FIG. 3. $\rho(T)/T^3$ as a function of T/T_c . Data have been obtained on a $48^3 \times L_t$ lattice, with variable L_t and at $\beta = 2.75$ (first 9 points), and variable β at $L_t = 4$ (last 10 points).

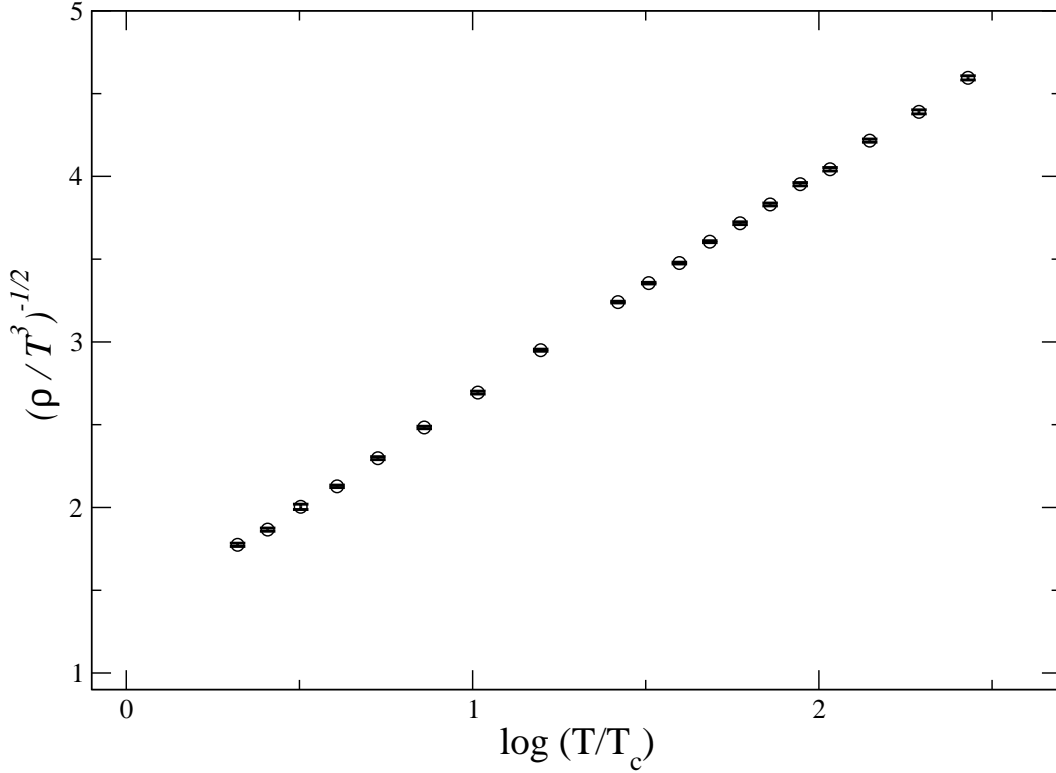


FIG. 4. $\sqrt{(\rho(T)/T^3)^{-1/2}}$ versus $\log(T/T_c)$. The data are the same reported in Fig. 3. The linear dependence is manifest.

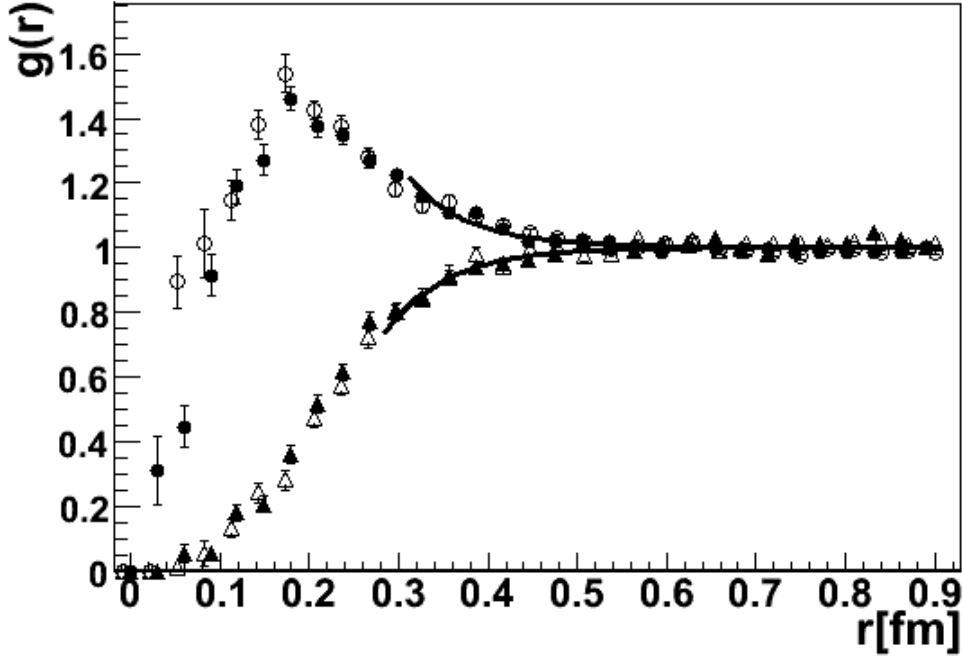


FIG. 5. $g(r)$ for the monopole-monopole (triangles) and the monopole-antimonopole (circles) case and for two different lattice sizes and β values corresponding to the same physical volume and temperature ($T \simeq 2.85 T_c$): $40^3 \times 5$ at $\beta = 2.7$ (empty markers) and $64^3 \times 8$ at $\beta = 2.86$ (full markers). The reported curves correspond to fits according to $g(r) = \exp(-V(r)/T)$ with $V(r)$ a Yukawa potential (see Eqs. (2.9) and (2.10)).

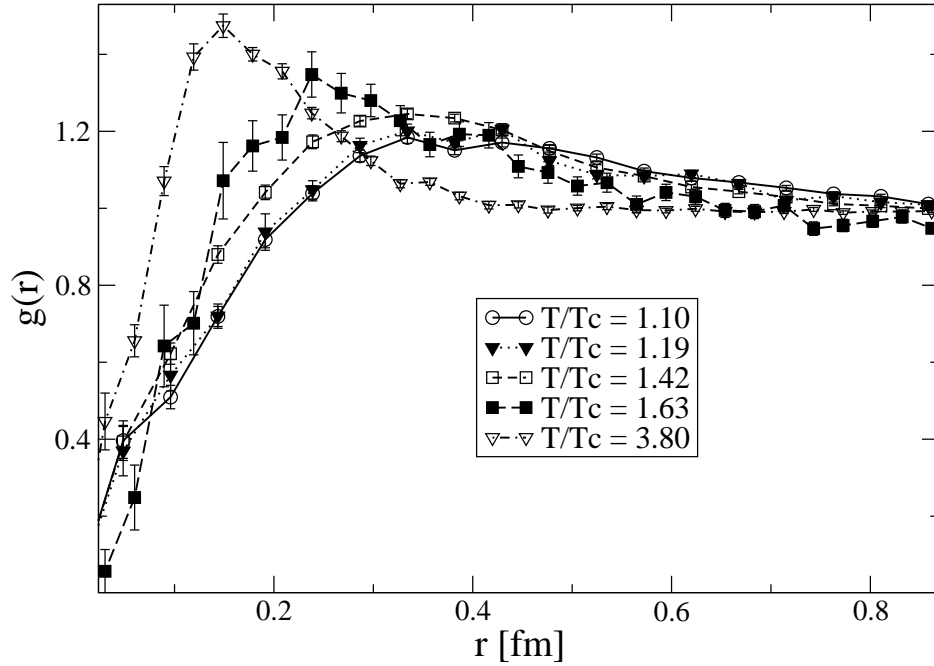


FIG. 6. $g(r)$ in the monopole-antimonopole case determined for different values of the temperature T .

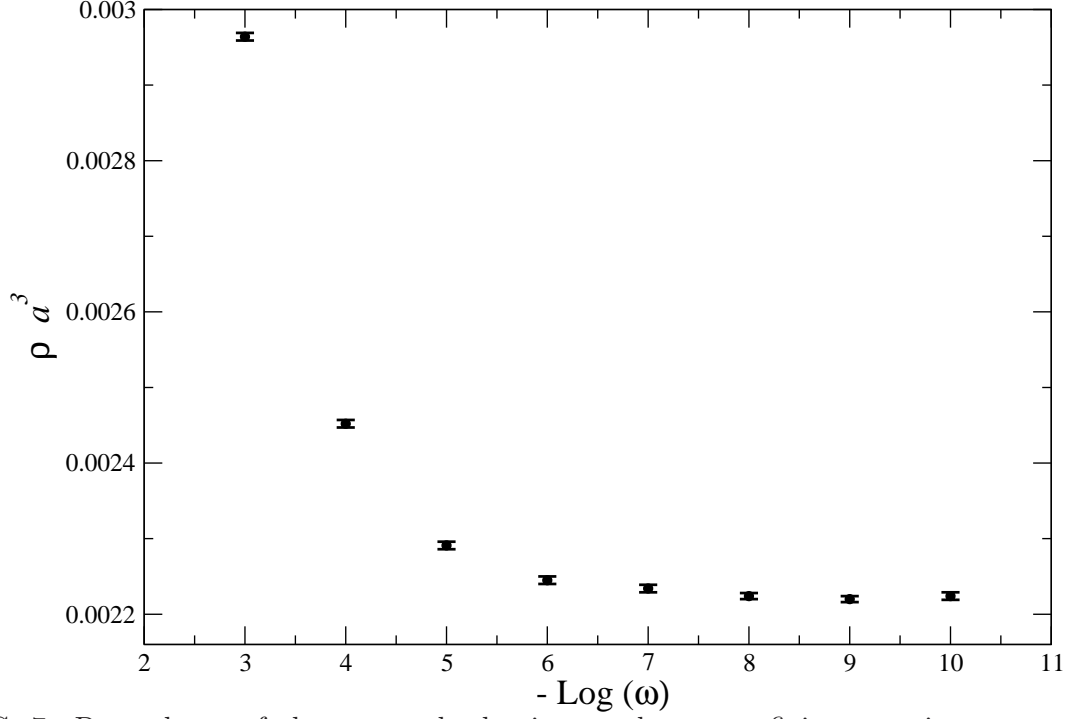


FIG. 7. Dependence of the monopole density on the gauge fixing stopping parameter for $L_s = 32$, $L_t = 4$ and $\beta = 2.6$.

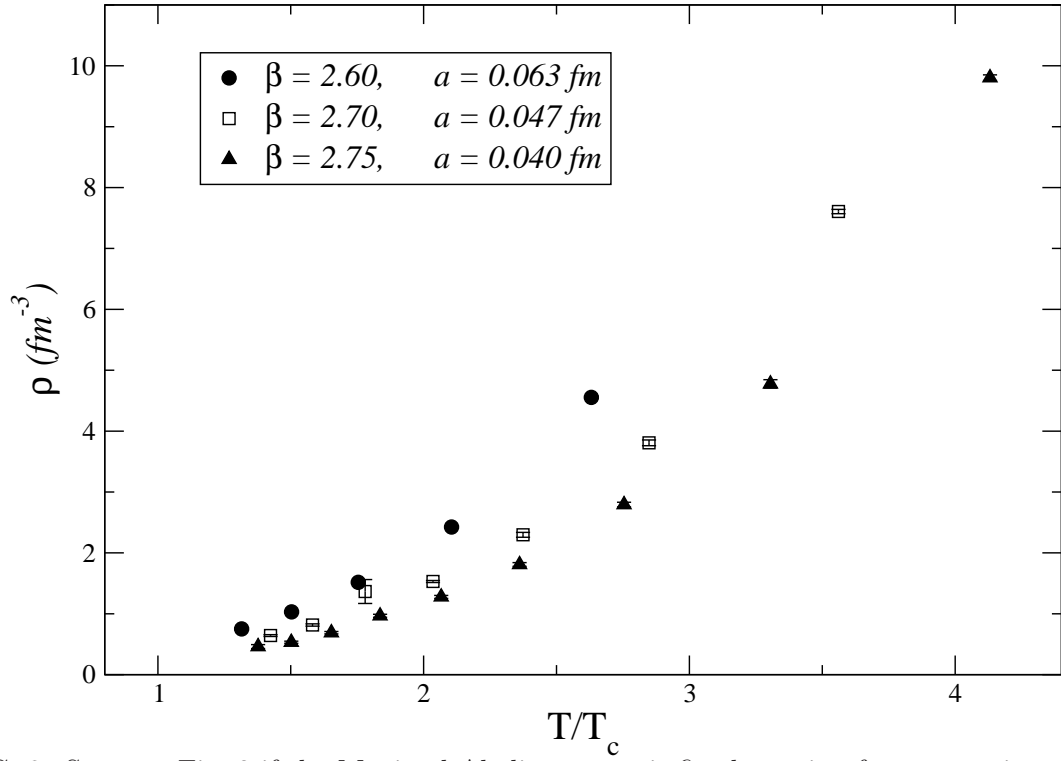


FIG. 8. Same as Fig. 2 if the Maximal Abelian gauge is fixed starting from a maximum of the Landau functional.